Influence of Molecular Weight on Impact Fracture Behavior of Injection Molded High Density Polyethylene: Scanning Electron Micrograph Observations

Bin Li, Guan Gong, Bang-Hu Xie, Wei Yang, Ming-Bo Yang

College of Polymer Science and Engineering, State Key Laboratory of Polymer Materials Engineering, Sichuan University, Chengdu 610065, Sichuan, People's Republic of China

Received 12 November 2007; accepted 19 January 2008
DOI 10.1002/app.28143
Published online 15 April 2008 in Wiley InterScience (www.interscience.wiley.com).

ABSTRACT: A group of high density polyethylene with different molecular weight was prepared by melt blending two kinds of HDPE with weight average molecular weight of 3.2×10^5 g/mol and 7.2×10^5 g/mol, respectively. The fracture behavior of injection molded specimens of these samples was investigated by Izod impact test and scanning electron microscopy. The results show that the variations of impact toughness of injection molded HDPE could be reflected directly by the evolution of morphology of fracture surface as molecular weight increases. Higher molecular weight led to higher impact toughness, due to both thickened oriented shear zone which could enhance the crack resistance and depressed two types of fracture behavior (tearing-brittle fracture and heat softening/melting fracture) with low energy consumption. Fracture behavior in different position of injection molded HDPE shows different molecular weight dependence. The impact toughness at far-gate-end increases with increasing molecular weight, while the impact toughness at near-gate-end, especially for the blends, almost keeps constant within a certain range of molecular weight. © 2008 Wiley Periodicals, Inc. J Appl Polym Sci 109: 1161–1167, 2008

Key words: HDPE; injection molding; molecular weight; fracture behavior; scanning electron micrograph

INTRODUCTION

The hierarchical structures always exist in injection molded polymers and their composites, which are codetermined by flow and crystallization behavior of polymer melt, compatibility between polymer matrix and dispersed phases, as well as processing conditions, such as melt temperature, injection speed, holding pressure, and so on.[1–8] For amorphous polymers, the hierarchical structures were greatly resulted from different molecular orientation along both flow direction and thickness, generated by melt flow.[2] For crystalline polymers, owing to the complex crystal structures appeared in injection molded specimens, greater efforts were taken to study morphology of injection molded semicryalline polymer and its mechanical properties in past few years.[1–12]

In injection molded semicrystalline polymers,[8,13–15] the crystal structures vary along both the flow direction and the thickness direction (i.e., the direction perpendicular to the melt flow). From the surface to the center of the specimen, the thickness direction could generally be partitioned to three sections, i.e., skin layer and shear zone with highly oriented lamellae along flow direction, as well as core layer with nonoriented spherulites. In addition to the spherulites and lamellae structures, the shish-kebab structures were also observed in injection molded polypropylene and polyethylene caused by shear-induced crystallization during injection molding.[4,5,14,16] On the other hand, in flow direction, the orientation of molecule chains and crystals, the thickness of the three layers mentioned above and other microstructures also undergo gradual changes.[8] External conditions significantly affect the morphologies of injection molded parts. Pantani et al.[3] found that higher holding pressure could promote molecular orientation in polypropylene mainly due to increased relaxation time under higher pressure. Furthermore, the thickness of specimens[2,4] and injection speed[2] also influenced the orientation inside injection molded parts in different ways, whereas the mold temperature ranging from 20 to 40°C, seemed to have little effect on molecular orientation.[2] Viana[7] pointed out that the thickness of skin layer increased with the decrease in melt temperature and injection flow rate, and similar phenomenon was also found in Nylon 6 by Murthy et al.[17] It

Correspondence to: B. H. Xie (xiebangh@tom.com).
Contract grant sponsor: National Natural Science Foundation of China; contract grant number: 10590351.
Contract grant sponsor: Special Funds for Major Basic Research; contract grant number: 2005CB623808.

©2008 Wiley Periodicals, Inc.
WILEY InterScience® DISCOVER SOMETHING GREAT

is well acknowledged that high molecular orientation and shish-kebab structures are beneficial to mechanical performance of semicryalline polymers. Thus some novel injection molding techniques were developed to produce these structures, such as, high pressure injection molding,[18] elongation flow molding,[19] and so on. Shen and coworkers[11,12,20,21] accomplished injection molding in oscillating/vibration stress field under low pressure to promote higher molecular orientation and the formation of shish-kebab structures, which endowed the products with excellent mechanical properties.

During fracture process, different crystal structures fracture in different manners corresponding to varying energy consumption, thus it is convenient and efficient to investigate fracture performance and deformantion mechanism of injection molded semicrystalline polymer by directly analyzing the morphology of fracture surface. Some attentions have been paid to this field,[6,15,22–25] especially in polymer composites.

As well known, molecular weight (MW) strongly affects mechanical properties of polymers. Fracture and deformation behavior of polymers with various MW have also been extensively studied.[25–28] The toughness of polymers could be improved with increasing MW. In the meanwhile, it can be expected that the improved fracture toughness derives from changes of fracture behavior caused by growth of MW.

Injection-molded high density polyethylene (HDPE) has been widely applied for decades; however, the relationships between morphology and properties of injection molded HDPE were less discussed in past few years. Lapique et al.[15] studied the relationship between morphology and fracture behavior of HDPE with weight average MW lower than 2×10^5 g/mol. Sousa et al.[29] investigated the relationships of MW, fracture morphology, and physical properties of HDPE in shear-controlled orientation in injection molding. HDPE and its composites via vibration-injection-molding also showed remarkable relationship between the morphology and mechanical properties.[5,11,12,20,21]

The main objective of this paper is to study how MW affects fracture toughness of injection molded HDPE from the point of view of morphology of fracture surface. Furthermore, for a better understanding of the effect of MW on the fracture behavior of different parts of injection molded HDPE, the fracture behavior of both far-gate-end and near-gate-end were studied.

To investigate fracture behavior of injection molded HDPE with different MW, two HDPEs with different MW were melt-blended on an extruder to prepare a set of HDPE with continuous MW in the range of 3.2×10^5 to 7.2×10^5 g/mol. The impact fracture toughness of both far-gate-end and near-gated-end was tested, and the fracture behavior of them was investigated on the basis of morphology of fracture surface observed with scanning electron microscopy (SEM). Since the skin layer occupies relatively small portion of the thickness of the injection molded specimen and consequently consumes less energy during fracture, the fracture behaviors of shear zone and core layer are the emphases of this study. The relationships between MW, fracture behavior and impact fracture toughness were discussed.

MATERIALS AND EXPERIMENTS

Two kinds of HDPE applied in this study are 5300B granules with the weight average MW of 3.2×10^5 g/mol (DaQing Petrochemical) and DMD1158 powder with the M_w of 7.2×10^5 g/mol (QiLu Petrochemical). Owing to the inferior mobility of DMD1158 melt, two HDPEs and their blends were extruded and palletized twice to promote mixing on a corotating twin-screw extruder (TSSJ-25, Chenguang Chemical Institute, China) with a temperature profile ranging from 160 to 210°C. The mass ratio of 5300B/DMD1158 was set as 100/0, 70/30, 50/50, 30/70, and 0/100, respectively. The granules obtained by twice extrusion were injected into rectangular bars (width× thickness of 10.2 mm × 4.2 mm) at a melt temperature of 230°C, injection speed of 10.8 cm^3/s, holding pressure of 43.2 MPa, and holding time of 20 s. About 24 h after the injection molding process, 2-mm deep V-shape notches of the specimens at the same side of both the far-gate-end and near-gate-end of injection molded specimens were cut. The scheme of the test specimen is shown in Figure 1.

The impact test was performed on an Izod impact tester. The morphology of the fracture surface of these injection-molded specimens were observed by SEM (JSM-5900LV, JEOL), with an accelerating voltage of 20 kV.

RESULTS AND DISCUSSION

The results of impact test are listed in Table I. It should be pointed out that the specimens of DMD1158 were not fractured by impact loading, thus the real impact toughness of DMD1158 should be much higher than the values in Table I. Furthermore, owing to the larger residual width of the specimens at-far-gate-end, the discrepancy of the impact between both ends would be enlarged.

Morphology of the fracture surfaces at far-gate-end

Figure 2 presents the morphology of the fracture surface of 5300B at the far-gate-end and its magnified

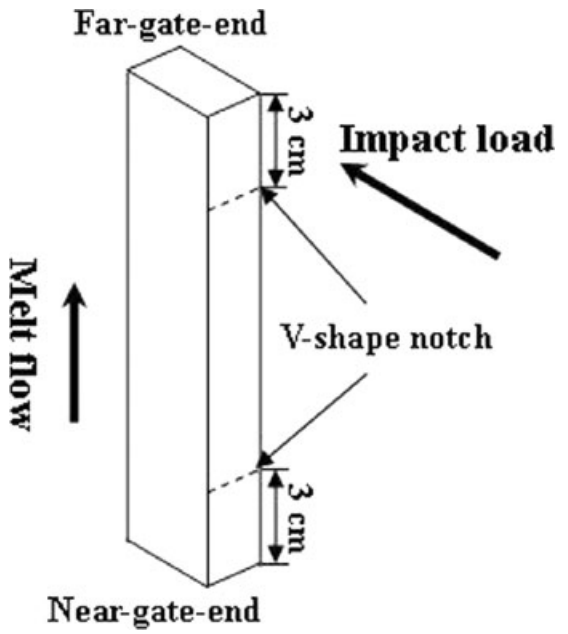

Figure 1 Scheme of the specimen applied in Izod impact test.

images in different fracture regions. According to the full view of the fracture surface in Figure 2(A), three distinct morphologies of the fracture surface can be clearly observed, indicating the discrepant fracture behaviors of the spherulites in core layer

TABLE I
Impact Toughness of Injection-Molded HDPE at Far-Gate-End and Near-Gate-End

Mass ratio of 5300B/DMD1158	Impact toughness at far-gate-end (kJ/m^2)	Impact toughness at near-gate-end (kJ/m^2)
100/0	15.74	29.25
70/30	30.29	46.96
50/50	38.43	42.99
30/70	43.40	45.68
0/100	85.87[a]	62.31[a]

[a] The real impact toughness should be higher.

and the oriented lamellae in shear zone. In the core layer, the crack propagation begins with a kind of ''tearing-brittle'' fracture behavior, as shown in Figure 2(B). In this region, both extensive tearing structures and brittle fracture surface surrounded by these tearing structures can be observed. The fracture behavior in this area should be considered as one fracture mode of spherulites. The brittle fracture may possibly be associated with the crack propagation along spherulites surfaces[30] affected by the initial stress state of the notch tip. As crack propagates further, the spherulites in the core layer undergo crazing and fibrillation,[15] as shown in Figure 3(C) (at the magnification of $\times$3000), and this is different from fracture behavior in Figure 3(B). A great deal

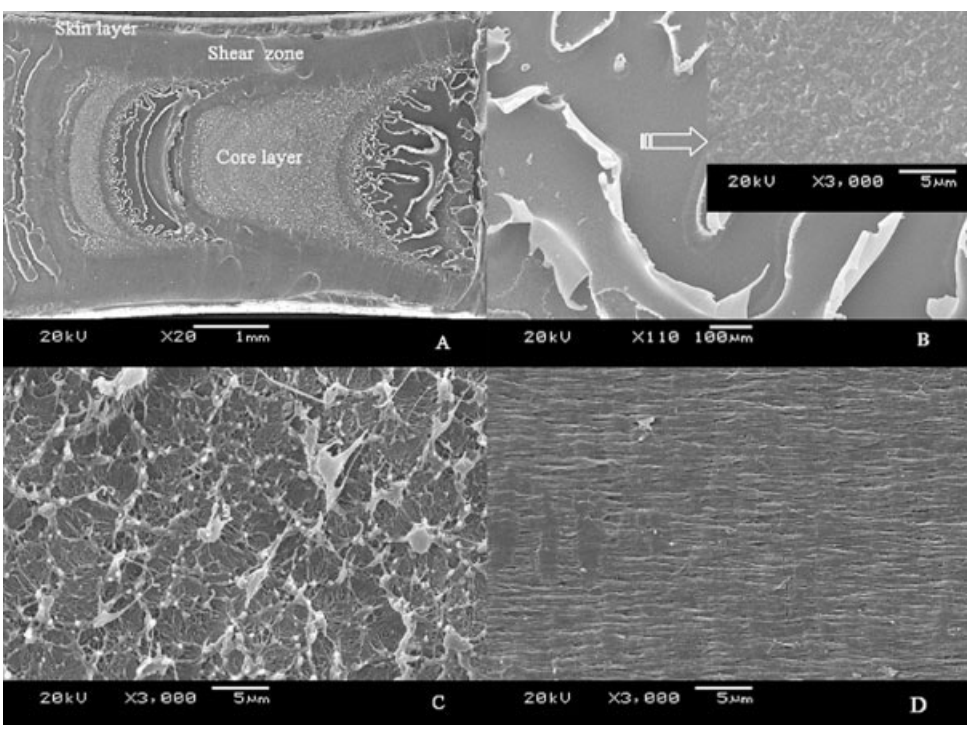

Figure 2 Scanning electron micrographs of fracture surface of 5300B(low molecular weight) at far-gate-end. (A) full view, (B) magnified view of tearing-brittle fracture surface in core layer, (C) magnified image of heat softening/melting fracture surface in core layer, (D) magnified image of shear zone.

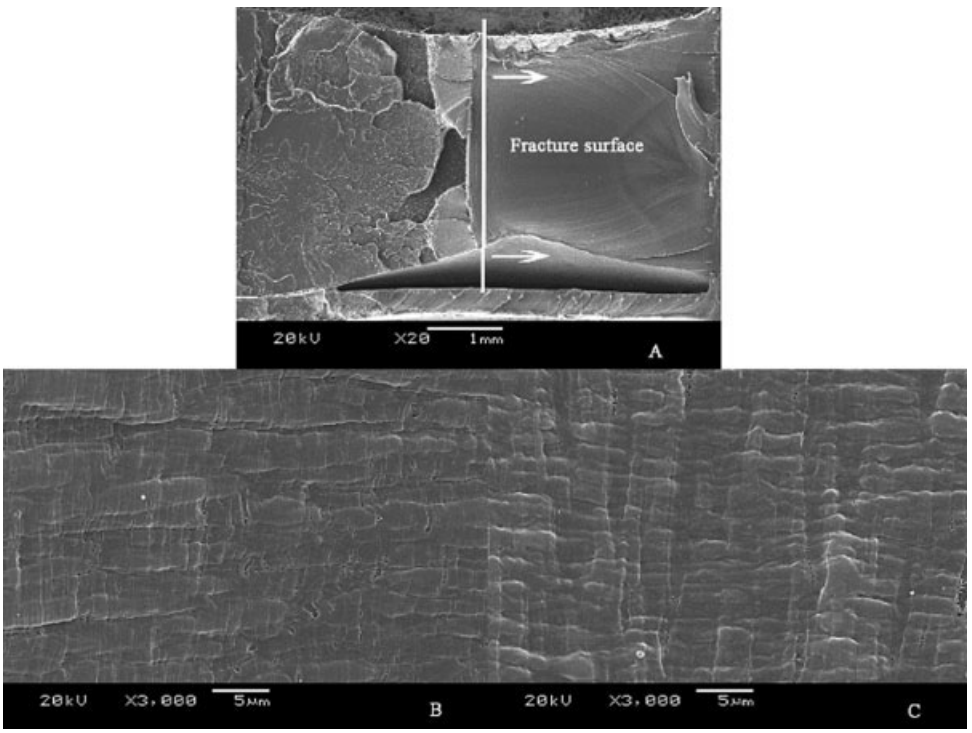

Figure 3 Scanning electron micrographs of fracture surface of DMD1158 (high molecular weight) at far-gate-end. (A) full view, (B,C) magnified image taken from shear zone and core layer respectively.

of filaments formed by stretching of the lamellae in spherulites, radiates from the bottom of the fracture surface with nodular-like knobs at the tips of the fibrils, which represents the occurrence of heat softening, or even melting of 5300B during fracture, and these knob structures are formed by the retraction of hot fibrils.[25] Such a fracture behavior is termed as ''heat softening or melting'' fracture behavior in this article and abbreviated as HSM. Since the heat softening and melting could impair the load carrying capacity of the deformed polymer, the stress could not be effectively transferred from one matrix surface to another. This facilitates the crack propagation and consequently decreases the fracture energy dissipated in this area. Then, the core layer of 5300B experienced another ''tearing-brittle'' fracture and HSM fracture before the complete fracture of the specimen. In the shear zone, the oriented lamellae fractured in the same manner [Fig. 3(D)] along the width direction, unlike the spehrulites in the core layer. The well-oriented tearing fibrils parallel to the impact loading direction could be distinctly observed without any heat softening or melting induced knob structures. Some publications[31,32] pointed out that the fracture of oriented shear zone needs more energy compared to core layer in injection molded specimens.

The high MW HDPE (DMD 1158) fractures in a totally disparate way showing a relatively homogeneous and intense bulk deformation without notable differences between the shear zone and core layer [Fig. 3(A)], contrasted with low MW HDPE (5300B, Fig. 2). The appearance throughout the fracture surface presents the stripe-like features oriented along the loading direction [Fig. 3(B,C)], although some dissimilarities of stripe-like features still exist between shear zone and core layer. Such a fracture behavior indicates the prevailing strain hardening phenomenon[25] strongly affected by the growth of MW, in which more HDPE is dragged into deformation zone during the fracture process and consequently the toughness is enhanced.[31] On the other hand, as the MW increases, the heat softening or melting phenomenon is depressed. According to a closer observation of Figure 3(B,C) taken from the marked positions in Figure 4(A), it is found that there are no visible structures of fractured spherulites or lamellae as shown in Figure 2, possibly owing to the hampered fibrillation process and enhanced plastic deformation occurring at the crystal boundaries[29] induced by increased interspherulitic or interlamellar tie chains for high MW HDPE.

Figure 4 shows the micrographs of the fracture surface of injection-molded specimens of the blends at the far-gate-end. In Figure 4(A), the addition of DMD1158 enlarges the thickness of shear zone as expected,[31] that is, the high MW component (HWMC) could improve the formation of the ori-

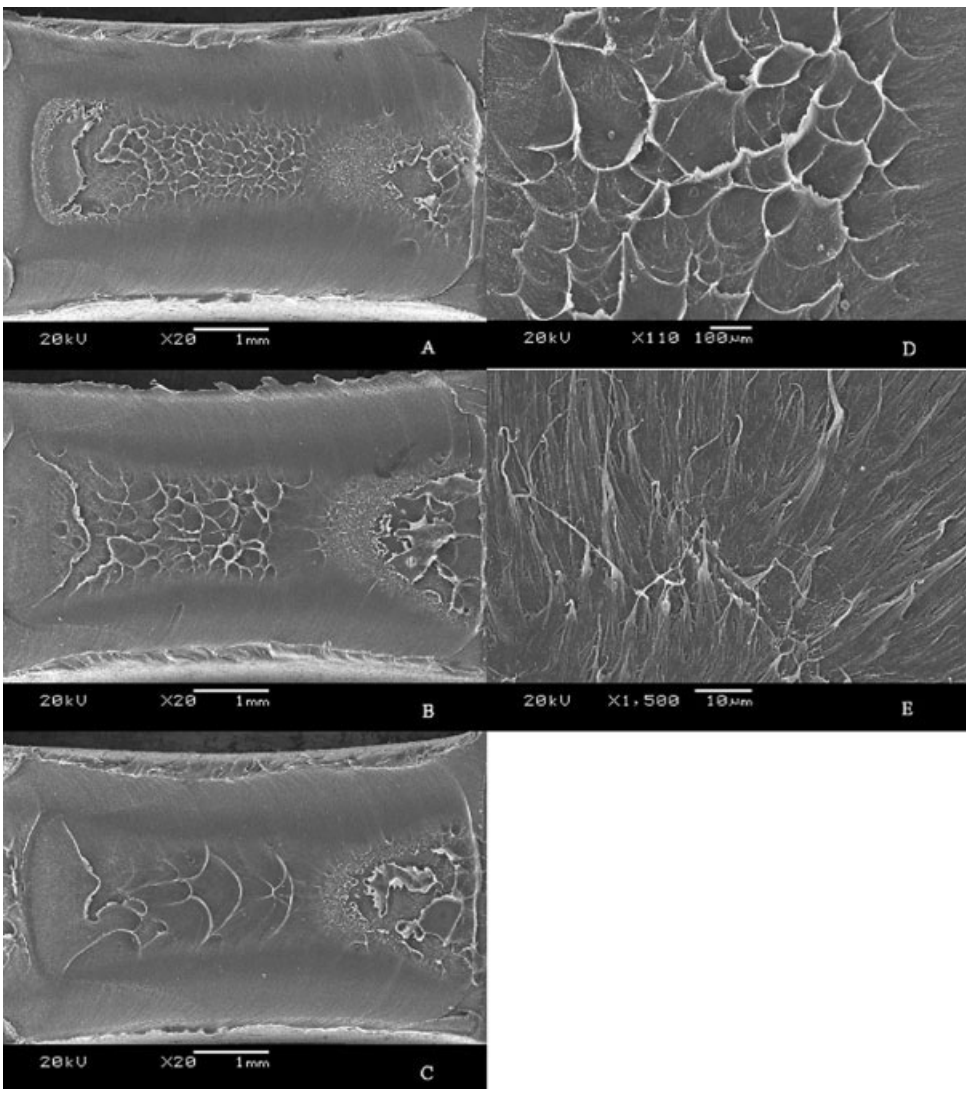

Figure 4 Scanning electron micrographs of fracture surface of the blends at far-gate-end mass ratio of 5300B/DMD1158: (A) 70/30, (B) 50/50, (C) 30/70, (D,E) magnified image of crater-shape structure taken from (A).

ented lamellae during the injection molding. However, it is interesting that the increasing content of HWMC seems to have little effect on thickening shear zone. The thickness of the shear zone almost keeps constant about 1 mm. On the other hand, the fracture behaviors in the core layer are dramatically affected by the addition of HWMC and its increasing content. With the addition of HWMC from 30 to 70 wt %, besides the restriction of tearing-brittle fracture, the HWMC also leads to the depression and even vanishing of the HSM fracture like that shown in Figure 2(C). Both structure changes indicate that more spherulites are involved in the plastic deformation, i.e., the gradual prevailing of strain hardening, which results in increased fracture energy consumption. Instead of the HSM fracture structures [Fig. 2(C)], the addition of HWMC promoted the formation of a great number of crater-shape deformation unit with well defined round borders, as shown in Figure 4(D) taken from the marked position in Figure 4(A). In this structure [Fig. 4(D,E)], a great number of fibrils radiates from a center at the bottom of the surface, without the knob-like structures attached at the tips of the fibrils. As the content of HWMC increases, the amount of the crater structures decreases, along with the enlarged size of them. When the content of DMD1158 reaches 70 wt %, the deformation units are too big to be distinguished except the arc-shape borders. The changes of crater-shape structures suggest the enhanced strain hardening and restrained HSM phenomenon with the further growth of MW. In summary, the evolution of fracture behavior, i.e., the gradually prevailing of strain hardening and the broadening of shear zone, accounts for the enhancement of impact toughness (Table I), as the MW of HDPE increases.

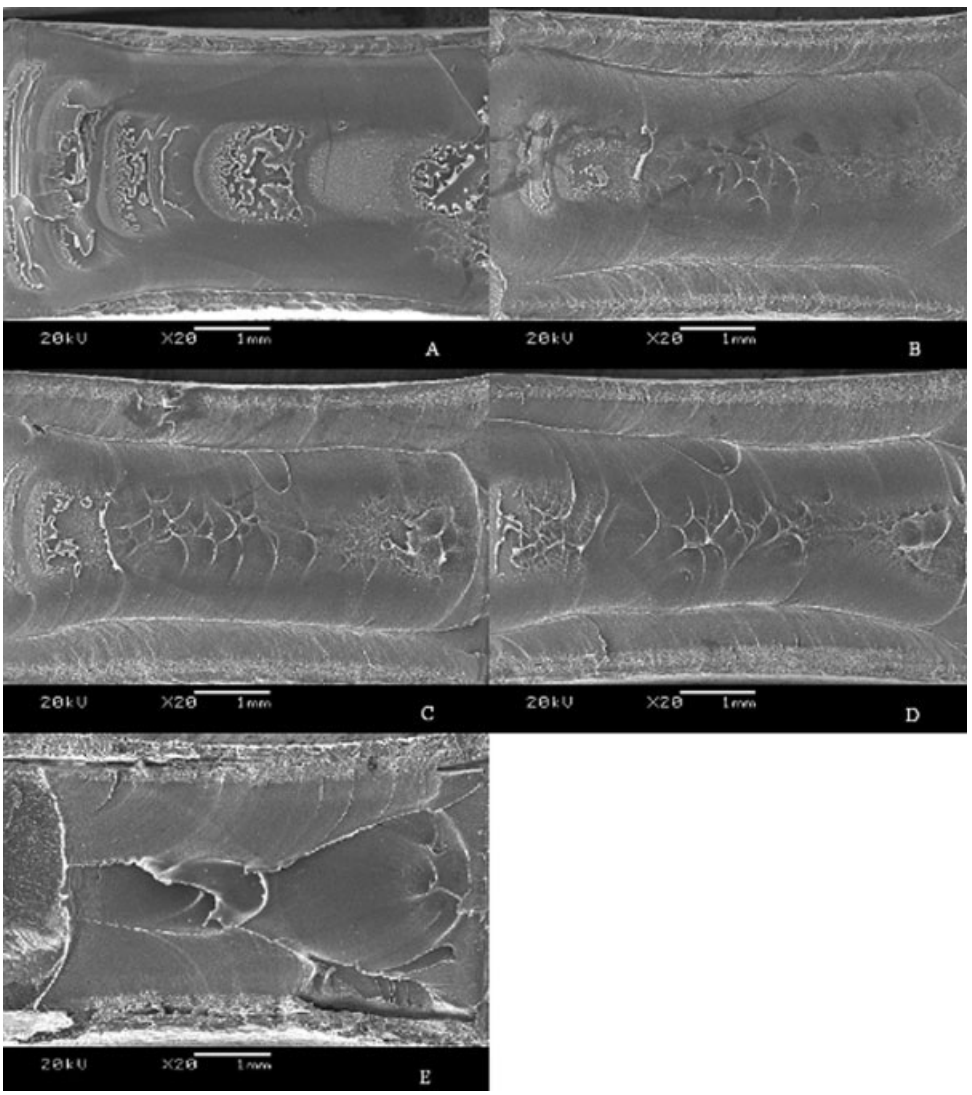

Figure 5 Scanning electron micrographs of fracture surface of two HDPEs and their blends at near-gate-end, mass ratio of 5300B/DMD1158: (A) 100/0, (B) 70/30, (C) 50/50, (D) 30/70, (E) 0/100.

Morphology of the fracture surfaces at near-gate-end

Owing to the evolution of the microstructures such as crystallinity, skin-core configuration, and so on, along the flow direction, the fracture behavior shows discrepancies between near-gate-end and far-gate-end, and furthermore, the dependence of fracture behavior of both ends on MW is also different.

For 5300B [Fig. 5(A)], compared with the morphology of the fracture surface at the far-gate-end, the fracture surface at near-gate-end shows much thicker shear zone as well as small regions of evidently restricted HSM fracture and brittle-tearing fracture, indicating that the injection molded specimen at near-gate-end shows better crack resistance. This is why the specimen of 5300B has much better impact toughness at near-gate-end. Based on this explanation, it is easily understood why the injection molded specimens of the blends [Fig. 5(B,D)] is tougher at near-gate-end.

Attributed to the addition of HWMC, like the far-gate-end, both the HSM fracture and brittle-tearing fracture in the core layer are dramatically restricted, at the same time, two ridges appeared in broader shear zones consisting of similar oriented fibrils as in Figure 2(D). However, the increasing content of HWMC did not induce remarkable changes of the fracture behavior of injection molded specimens of the blends at the near-gate-end [Fig. 5(B,D)], which resulted in almost the same impact fracture toughness about 45 kJ/m^2. On the other hand, the disparities of fracture behavior between both ends are gradually narrowed with increasing content of HWMC, in agreement with that of impact toughness. When the mass percent of DMD1158 is 70 wt %, the impact toughness of both ends is approximately

equal to each other resulted from the similarity of the fracture behavior of both ends [Figs. 4(C) and 5(D)].

Throughout the fracture surface of DMD1158 [Fig. 5(E)], the intense ridge-shaped deformation zone consisting of similar stretched fibrils as shown in Figure 2(D), can be observed, probably indicative of the better mobility and deformability of the crystals during fracture with regard to the far-gate-end, which accounted for inferior fracture impact toughness at the near-gate-end of DMD1158. In addition, this fracture behavior is also responsible for the formation of ridge structures in the shear zone shown in Figure 5(B,C).

CONCLUSIONS

1. MW influences fracture behavior of injection molded Hdpe in two ways:
   First, the growth of MW depresses tearing-brittle fracture behavior and heat softening/melting fracture behavior, both of which lead to low energy consumption and prevail in HDPE with low MW. For HDPE with high MW, strain hardening is the dominant phenomenon occurring in the process of fracture.
   Second, high MW favors the formation of shear zone during melt filling, which possesses better crack resistance compared to the nonoriented core layer; however, with increasing addition of high MW component in the blends, the thickness of the shear zone is insensitive to the variation of MW.
2. The impact toughness show great coincidence with fracture behavior (morphology of fracture surface) at both the far-gate-end and the near-gate-end. According to the observations of fracture surface, the variations of impact toughness at both ends can be well explained.

References

1. Zhong, G. J.; Li, Z. M. Polym Eng Sci 2005, 45, 1655.
2. Mendoza, R.; Régnier, G.; Seiler, W.; Lebrun, J. L. Polymer 2003, 44, 3363.
3. Pantani, R.; Coccorullo, I.; Speranza, V.; Titomanlio, G. Polymer 2007, 48, 2778.
4. Zhu, P. W.; Edward, G. Polymer 2004, 45, 2603.
5. Guan, Q.; Lai, F. S.; Mccarthy, S. P.; Chiu, D.; Zhu, X. G.; Shen, K. Z. Polymer 1997, 38, 5251.
6. Karger-Kocsis, J.; Mouzakis, D. E. Polym Eng Sci 1999, 39, 1385.
7. Viana, J. C. Polymer 2004, 45, 993.
8. Pantani, R.; Coccorullo, I.; Speranza, V.; Titomanlio, G. Prog Polym Sci 2005, 30, 1185.
9. López, L. C.; Cieslinski, R. C.; Putzig, C. L.; Wesson, R. D. Polymer 1994, 36, 2331.
10. Fujiyama, M.; Masada, I.; Mitani, K. J Appl Polym Sci 2000, 78, 1751.
11. Zhang, J.; Shen, K. Z.; Gao, Y. G.; Yuan, Y. J Appl Polym Sci 2005, 96, 818.
12. Lei, J.; Jiang, C. D.; Shen, K. Z. J Appl Polym Sci 2004, 93, 1591.
13. Aurrekoetxea, J.; Sarrionandia, M. A.; Urrutibeascoa, I.; Maspoch M. L. L. Polymer 2003, 44, 6959.
14. Stern, C.; Frick, A.; Weickert, G. J Appl Polym Sci 2007, 103, 519.
15. Lapique, F.; Meakin, P.; Feder, J.; Jøssang, T. J Appl Polym Sci 2000, 77, 2370.
16. Zheng, G. Q.; Huang, L.; Yang, W.; Yang, B.; Yang, M. B.; Li, Q.; Shen, C. Y. Polymer 2007, 48, 5486.
17. Murthy, N. S.; Kagan, V. A.; Bray, R. G. Polym Eng Sci 2002, 42, 940.
18. Boldizar, A.; Månson, J. A.; Rigdahl, M. J Appl Polym Sci 1990, 39, 63.
19. Bayer, R. K.; Zachmann, H. G.; Baltá Calleja, F. J.; Umbach, H. Polym Eng Sci 1989, 29, 187.
20. Zhang, G.; Fu, Q.; Shen, K. Z.; Jian, L.; Wang, Y. J Appl Polym Sci 2002, 86, 58.
21. Liang, S.; Wang, K.; Yang, H.; Zhang, Q.; Du, R. N.; Fu, Q. Polymer 2006, 47, 7115.
22. Van der zwet, M. J. M.; Heidweiller, A. J. J Appl Polym Sci 1998, 67, 1473.
23. Mcevoy, R. L.; Krause, S. J Appl Polym Sci 1997, 64, 2221.
24. Bureau, M. N.; Di Francesco, E.; Denault, J.; Dickson, J. L. Polym Eng Sci 1999, 39, 1119.
25. Brough, I.; Haward, R. N.; Healey, G.; Wood, A. Polymer 2004, 45, 3115.
26. Wang, X. L.; Li, R. K. Y.; Cao, Y. X.; Meng, Y. Z. Polym Test 2005, 24, 699.
27. Zuiderduin, W. C. J.; Homminga, D. S.; Huétink, H. J.; Gaymans, R. J. Polymer 2003, 44, 6361.
28. Hillmansen, S.; Hobeika, S.; Haward, R. N.; Leevers, P. S. Polym Sci Eng 2000, 40, 481.
29. Sousa, R. A.; Reis, R. L.; Cunha, A. M.; Bevis, M. J. J Appl Polym Sci 2003, 89, 2079.
30. Perkins, W. G. Polym Eng Sci 1999, 39, 2445.
31. Schrauwen, B. A. G.; Breemen, L. C. A. V.; Spoelstra, A. B.; Govaert, L. E.; Peters, G. W. M.; Meijer, H. E. H. Macromolecules 2004, 37, 8618.
32. Zuidema, H.; Peters, G. W. M.; Meijer, H. E. H. Macromol Theory Simul 2001, 10, 447.